Stability of three-dimensional electron holes

M. Berthomier,[1,a)] G. Dubois,[2] and L. Muschietti[3]
[1]*Centre d'Étude des Environnements Terrestre et Planétaires, UMR 8639, CNRS-UVSQ/IPSL, 10-12 Avenue de l'Europe, F-78140 Vélizy, France*
[2]*Laboratoire Kastler-Brossel, Ecole Normale Supérieure, 24 rue Lhomond, 75005 Paris, France*
[3]*Space Sciences Laboratory, University of California, Berkeley, 7 Gauss Way, Berkeley, California 94720, USA*

(Received 7 April 2008; accepted 13 October 2008; published online 12 November 2008)

A self-consistent kinetic model of three-dimensional (3D) electron holes in a strongly magnetized collisionless plasma is presented. A stability study of these localized electrostatic structures has been carried out. The analysis of the motion of trapped particles in the 3D potential structure suggests using the Hamiltonian approach to describe how electron holes interact with an external electrostatic perturbation. Using 3D action-angle variables and perturbation theory, it is shown that, in addition to standard Landau resonance of passing (i.e., untrapped) particles, trapped particles resonate with the perturbation in such a way that they amplify it. A growth rate for this process is derived and application to magnetospheric plasma conditions shows that the stability of 3D electron holes is strongly dependent on the anisotropy of the underlying potential structure. Possible production of electrostatic whistler waves by a train of electron holes in the auroral region of the Earth's magnetosphere is emphasized. © *2008 American Institute of Physics*. [DOI: 10.1063/1.3013452]

I. INTRODUCTION

Observations by the Fast Auroral SnapshoT (FAST) satellite[1] have revealed the existence of fast solitary structures in Earth's auroral regions.[2] They are transient electric field pulses associated with intense magnetic field-aligned electron fluxes and they are most frequently detected in the downward current region of the aurora above 2000 km altitude. They travel roughly at the electron drift velocity (a few thousand km/s) along the magnetic field **B** and their duration is $\sim 100\ \mu$s. They are similar to the structures identified in the plasma sheet boundary layer by the GEOTAIL satellite[3] since they appear as brief but intense emissions of broadband quasielectrostatic noise in power-frequency-time spectrograms. They have been also spotted at the magnetopause and at bow shock crossings by the POLAR and CLUSTER spacecraft.[4,5] They correspond to positively charged Debye-scale-length potential structures which are surrounded by a negative halo such that they are, on the whole, charge neutral. In auroral regions, their peak electric potential amplitude can be tens of percent of the parallel electron temperature and their peak electric field can reach 2.5 V/m.[2] They carry an energy up to $\sim 1\%$ of the thermal energy, which is typical of strong plasma turbulence. Their large amplitude and velocity, their positive polarity, and the fact that they carry no significant net potential drop along the magnetic field distinguishes them from the weak double layers[6] or ion-acoustic solitary waves[7] previously observed in association with the up-going ion beams of the upward current region of the aurora. However they are observed in or near regions of large amplitude quasistatic parallel electric fields.[2] Their potential structure in the parallel direction appears to be Gaussian since the electric field signatures fit well to the corresponding derivative. The parallel and perpendicular electric fields take the form of bipolar and monopolar spikes, respectively, which suggest that they are 2D or 3D structures. These fast solitary structures are similar to those observed by the POLAR spacecraft at higher altitudes in the polar cap.[8,9] Using a statistical analysis of this data set covering a wide range of altitudes, Franz *et al.*[10] have shown that the ratio of their perpendicular to parallel elongation relative to the magnetic field varies as $\sqrt{1+\omega_{pe}^2/\Omega_{ce}^2}$, where ω_{pe} and Ω_{ce} are the electron plasma frequency and gyrofrequency, respectively.

The observed fast solitary waves and the corresponding broadband spectra cannot be explained in the framework of linear plasma theory. Several nonlinear models have therefore been developed. They are two classes of such models. First, topological solitons and more specifically electron acoustic solitons models try to reproduce the characteristics described above. The linear electron acoustic wave only exists when two electron populations are present in the plasma with different temperatures and an appropriate hot-to-cold density ratio.[11] The limited parameter range in which the linear wave can exist puts some constraint on the existence of nonlinear electron acoustic solitons. These solitons result from the balance between the waveform steepening of the wave due to nonlinear terms in fluid equations and the dispersion which affects the acoustic wave propagation at Debye-length scales. Classical electron acoustic solitons correspond to negatively charged clouds[12] but the introduction of an electron beam leads to the appearance of positively charged electron acoustic solitons.[13] The velocity and amplitude along the magnetic field of the fast solitary structures can be explained by these 1D models but in the small-amplitude limit, the width of elecron-acoustic solitons is decreasing with amplitude for a given set of plasma parameters. This relationship is not observed in statistical studies of the parallel width and amplitude of solitary waves from FAST

a)Electronic mail: Matthieu.Berthomier@cetp.ipsl.fr.

(Ref. 14) and POLAR (Ref. 15) spacecraft. These studies instead show that the width of solitary waves increases with amplitude. It has also been shown that small-amplitude 3D electron-acoustic beam solitons can form in an electron-beam plasma system.[16] The role of particle drift across the magnetic field is essential in this model. Electrons are shown to perform an azimuthal and quasiperiodic motion across **B** due to the "$\mathbf{E}\times\mathbf{B}$" drift associated with the potential structure. This fluid model is consistent with the altitude distribution of the ratio of the perpendicular and parallel scale of the fast solitary waves but as in the 1D case, it fails reproducing width-amplitude relationships. Furthermore, these fluid models do not take into account trapped electrons and they do not describe the bounce motion of particles at sub-Debye length scales in the electrostatic potential structure, which is a major limitation.

Second, there has been a number of fast solitary wave models based on Bernstein–Green–Kruskal (BGK) modes.[17] BGK modes are stationary solutions of the Vlasov–Poisson equations in a moving reference frame. In the past, these nonlinear models have been introduced in order to understand laboratory observations of solitary waves.[18,19] In the context of fast solitary waves, a specific form of the BGK mode has been used in which the equilibrium is maintained by the electron dynamics while the ions form a homogeneous neutralizing background.[20,21] Electrons of negative total (kinetic and potential) energy are trapped inside the positive potential hump associated with the solitary wave while electrons with positive energy are just passing through the structure. These BGK modes take the form of localized phase space electron density holes: untrapped electrons are depleted in the center of the structure in order to compensate for the repulsion of accumulated trapped electrons in this region. The way a BGK mode is constructed is somewhat arbitrary since it is possible either to prescribe the functional form of the trapped and untrapped distribution function and to obtain the resulting potential structure[22] or to prescribe the untrapped distribution function and the shape of the potential structure in order to derive the self-consistent trapped distribution function.[23] This second method is well-suited to space plasma observations since present particle instrumentation is not fast enough to resolve trapped electron distribution functions on the millisecond time scale while the average untrapped distribution function can be measured on a slower time scale and the potential structure can be derived from electric field waveform measurements.[2] These models correctly reproduce the parallel properties of fast solitary waves. Depending upon the choice of the untrapped distribution function, some restrictions have been shown to exist on the parameters and waveforms of electron holes. These limitations resulting, for example, from the positiveness of the trapped distribution function imply that the minimum spatial width of the BGK mode should increase with its amplitude.[21] In the FAST data set, the observed width of solitary waves is close to this minimum value[14] while at POLAR altitudes, Chen *et al.*[24] showed that it can be significantly larger than this particular value. Other general relationships between electron hole parameters can be derived[25] but in most cases they rely on small amplitude developments that are not justified in the case of the large amplitude fast solitary waves that we deal with here. A full 3D BGK model of fast solitary waves has also been developed[26] and will be presented and generalized in this paper in order to self-consistently take into account the finite velocity of electron holes in the derivation of the trapped distribution function.

The question of stability of 3D electron holes can be tackled either by considering the evolution of the nonlinear structure from the very beginning of its generation or by introducing large amplitude electron holes in a simulation and by looking at its robustness against longitudinal or transverse perturbations. The simulations have shown that electron holes emerge from the strongly nonlinear interaction between bidirectional electron beams.[27] They also appear in 1D current-driven systems with a seed local density inhomogeneity: a potential ramp forms at the site of the density fluctuation and it accelerates the electrons that subsequently interact with the nondrifting electrons of higher temperature which stagnate upstream (i.e., on the high-potential side of the ramp) leading to the formation of fast solitary waves correctly described by a 1D electron hole theory.[28] Most 2D simulations suggest that 1D electron holes are robust structures on hundreds of inverse plasma periods in strongly magnetized plasmas. Still, as demonstrated by particle-in-cell (PIC) simulations[29] and Vlasov simulations[28] with periodic boundary conditions, we cannot preclude a weak instability of the electron hole relative to specific types of electrostatic perturbations, namely, to electrostatic whistler waves (EWW). Furthermore, 3D simulations have shown that the eventual decay of phase space tubes was accompanied by the emission of lower-hybrid waves,[30,31] which is the low-frequency cutoff of EWW. This decay only appears at late times and the emitted waves form long filaments parallel to the ambient magnetic field.[32] Plasma magnetization (Ω_{ce}/ω_{pe}) also appears to be a major element when considering electron hole stability since electron hole become highly transitory in weakly magnetized plasmas.[33] All these results are in agreement with the direct simulation of an isolated 1D (Ref. 21) and 3D theoretically determined BGK mode,[34] which shows that large amplitude electron holes are robust structures in strongly magnetized plasmas, but are grossly unstable for conditions where the bounce frequency of the trapped electrons along the magnetic field line ω_b is larger than their gyrofrequency Ω_{ce}.[35] Therefore, in the highly magnetized auroral regions where $\Omega_{ce} \gg \omega_{pe} > \omega_b$, one would expect the electron holes to live for at least several bounce periods.

In this paper, we are interested in the process of destabilization of electron holes by electrostatic whistler waves (EWW) since it appears to be one of the few processes which can affect electron hole stability in a strongly magnetized plasma. These waves are commonly observed in auroral regions.[36] Their frequency range extends from the lower-hybrid frequency (ω_{lh} hereafter) up to the electron plasma frequency, the lower-hybrid wave being the low frequency and high perpendicular wavenumber limit of this mode. Their approximate fluid dispersion relation is $\omega^2=\omega_{\mathrm{lh}}^2+\omega_{pe}^2\cos^2\theta$, where θ is the angle between the wave vector **k** and the magnetic field **B**. Among these emissions is the well-

known auroral hiss which has both electrostatic and electromagnetic components. However, auroral hiss is believed to be generated by incoherent Cerenkov emission from intense fluxes of precipitating electrons[37] observed in the upward current region. Therefore auroral hiss is a typical feature of these upward current regions. One can also see EWW emitted from downward current regions, in the form of VLF saucers or V-shaped VLF hiss emissions seen on frequency-time spectrograms.[38,39] The frequency-time dependence of VLF saucers is due to their dispersion relation and to the localization of their source region.[40] Observations by the VIKING spacecraft have shown that up-going electrons were sometimes observed in conjunction with VLF saucers.[41] FAST observations have recently revealed that as much as 85% of VLF saucers were actually associated with up-going electron fluxes.[42] Ergun *et al.*[43] also found that 79% of the VLF saucer events associated with up-going electron fluxes had fast solitary waves on their emitting flux tubes and that the localization of the source region was extreme (less than 10 km in some cases). These experimental results motivated 1D (Ref. 44) and 2D (Ref. 45) numerical simulations in which phase space holes (in 1D) and phase space tubes elongated across the magnetic field (in 2D) where shown to emit EWW. While these simulations could potentially explain the strong localization of VLF saucers source regions in the case of 1D and elongated 2D electron holes, the question whether EWW might be efficiently generated by the 3D electron holes which are actually observed in the downward current region of the aurora and the stability of these 3D holes versus EWW perturbations is still an open question and the main motivation of the research we report here.

The paper is organized as follows: In Sec. II, the first self-consistent model of the 3D electron hole in strongly magnetized plasma is presented. Compared to previous attempts to construct 3D BGK modes,[26] our model self-consistently includes the drift velocity of the localized structure relative to the untrapped distribution function. We also describe the trapped particle motion in the self-consistent 3D BGK mode. In Sec. III, we describe the Hamiltonian formalism that we developed in order to study trapped particles dynamics. In Sec. IV, we use this formalism to study the effect of an external electrostatic perturbation (e.g., an EWW) on particle dynamics. In Sec. V we look at the global effect of the pertubation by averaging over phase space its effect on the trapped particles. We derive an expression for the growth rate of EWW. In Sec. VI, we give the main results of the numerical study that we performed in order to gain some insight on the stability of 3D fast solitary waves. Section VII sums up the main results presented in that paper.

II. 3D BGK MODEL OF ELECTRON HOLES

Following Muschietti *et al.*,[26] we assume that there exists a frame moving along **B** in which electrostatic potential and electron distribution are in a self-consistent steady state while ions form a neutralizing background. In this frame, a potential cylindrically symmetric around a centric magnetic field line is defined by

$$\Phi_0(x,y,z) = \Gamma h(z) a(r), \tag{1}$$

where $r=\sqrt{x^2+y^2}$ is the radius away from the centric line, z is the coordinate along **B**, and Γ is the amplitude of the structure. We use a Gaussian profile $h(z)=\exp(-z^2/2\Delta^2)$ along as well as across the magnetic field with $a(r)=\exp(-r^2/2\delta^2)$. The case of a planar structure is recovered with $\delta\to\infty$. We improve upon Muschietti *et al.*[26] by including a finite drift V of electron holes relative to passing (i.e., untrapped) electrons. As it will be seen in Sec. V, the stability of electron holes does depend on this relative drift. In this section, we use standard dimensionless units where length is normalized by the electron Debye length λ_{De}, velocity by the electron thermal velocity $v_e \equiv \sqrt{T_e/m}$, potential by T_e/e, and time by the inverse plasma frequency ω_{pe}^{-1}. In the electron hole frame, the flattop distribution function of passing electrons can be qualitatively approximated by

$$f_{p\pm}(W) = \frac{6\sqrt{2}}{\pi[8+(W^{1/2}\pm V)^6]}, \tag{2}$$

where $W=v_\parallel^2-2\Phi_0(z,r)$ is twice the electron parallel energy $E_\parallel$ and $\pm$ corresponds to the sign of the parallel electron velocity $v_\parallel$. The density of trapped electrons n_t is given by the Poisson equation which reduces to

$$\Delta\Phi_0(z,r) = n_t(z,r) + n_p(z,r) - 1, \tag{3}$$

where n_p is the density of passing electrons derived from Eq. (2). It is required to examine the electron orbits in order to understand how an electron population can self-consistently maintain such an equilibrium. Muschietti *et al.*[26] have shown that in a strongly magnetized plasma the electron behavior can be analyzed in terms of three basic motions occurring on three distinct time scales: the fast cyclotron motion on Ω_{ce}^{-1} time scale, the back and forth bounce motion of trapped particles along **B** on time scale ω_b^{-1}, and a slow azimuthal drift along a shell at constant radius R on time scale ω_γ^{-1}. These time scales follow the ordering

$$\Omega_{ce}^{-1} \ll \omega_b^{-1} \ll \omega_\gamma^{-1} \tag{4}$$

and the azimuthal drift is given by

$$\omega_\gamma(W,R) = -\frac{\Gamma}{\Omega_{ce}\delta^2}\langle h(z)\rangle a(R), \tag{5}$$

where $\langle h(z)\rangle$ is the average of $h(z)$ over the bounce motion of trapped particles with energy $E_\parallel$ on a given cylindrical shell of constant radius R. This slow drift across the magnetic field is nothing else than the "$\mathbf{E}\times\mathbf{B}$" drift due to the self-consistent perpendicular electric field and R is the gyrocenter's position. This ordering holds as long as the parallel distance covered by the electrons over a gyroperiod is short compared to the parallel scale length of the potential Δ and as long as the radial profile of the potential $a(r)$ varies little over an electron gyroradius ρ_L (i.e., $\rho_L \ll \delta$). Within these approximations which are well satisfied in the strongly magnetized auroral plasma, and as it will be shown in Sec. III, we have three constants of the motion which are the perpendicular energy $v_\perp^2$, the parallel energy, and the radius of the gyrocenter R.

As a consequence, the density of trapped electrons is defined on each shell R as

$$n_t(\Phi_0,R) = \int_{-2\Phi_0}^{0} \frac{f_t(W,R)}{(W+2\Phi_0)^{1/2}} dW, \tag{6}$$

where f_t is the distribution function of trapped electrons and R takes the role of a parameter. This equation is inverted with the help of Laplace transforms[21] such that

$$f_t(W,R) = \frac{1}{2\pi} \int_0^{-W} (-W-p)^{-1/2} \frac{d}{dp} n_t(p,R) dp, \tag{7}$$

where the range of possible energies differs on each shell with $-2\Gamma a(R) \leqslant W \leqslant 0$. The trapped electrons distribution can be decomposed into two terms, namely,

$$f_t(W,R) = f_{ts}(W,R) + f_{tp}(W), \tag{8}$$

where the first contribution f_{ts}, which comes from the potential term in Eq. (3), is given by

$$f_{ts}(W,R) = \frac{\sqrt{-W}}{\pi} \left(\frac{1}{\Delta^2} \left\{ 1 + 2 \log \left[\frac{\Gamma a(R)}{-4W} \right] \right\} + \frac{1}{\delta^2} (R^2/\delta^2 - 2) \right). \tag{9}$$

Inclusion of the finite velocity V in Eq. (2) modifies the second term f_{tp} due to the passing electrons density in Eq. (3). After performing the corresponding double integral in Eq. (7), we obtained

$$\begin{aligned} f_{tp}(W) = {} & [3 + (-2W)^{5/2} + 8W^2 - 8W(2 + V^2/2) \\ & + (-W)^{3/2}(15 + 2V^2) + \sqrt{-W}(10 + 3V^2/2 + V^4/2)]/ \\ & \{2\sqrt{2}\pi[1 + 2\sqrt{-W} - W + V^2/2][1 + 2(-W)^{3/2} + W^2 \\ & - V^2/2 + V^4/4 + 2\sqrt{-W}(1 + V^2/2) - W(3 + V^2)]\}. \end{aligned} \tag{10}$$

Figure 1 gives the total electron distribution function as a function of parallel velocity $v_\parallel$ at the center ($R=0$) of an electron hole defined by normalized values $\Gamma=0.4$, $\Delta=2.6$, and $\delta=2$. In the upper panel there is no relative velocity V between the plasma and the electron hole reference frame while $V=1$ in the lower panel. In each panel three cuts of the distribution function are displayed at different locations $z=(\Delta, 2\Delta, 3\Delta)$ along the magnetic field.

As mentioned by Chen *et al.*,[24,46] electron holes only exist if the trapped distribution function is non-negative everywhere in phase space. Since the minimum of the distribution corresponds to the bottom of the electron hole where $R=0$ and $W=-2\Gamma$, this condition of existence is equivalent to the inequality $f_t(-2\Gamma,0)>0$. As in the 1D case there is no 1-1 relationship between the amplitude and widths of 3D electron holes but there are some domains of existence for electron holes. Equation $f_t(-2\Gamma,0)=0$ defines the bounding surface of these domains in the parameter space involving the amplitude (Γ), the velocity (V), the perpendicular (δ), and the parallel (Δ) width of 3D electron holes. While the detailed study of these surfaces is beyond the scope of this paper, we notice that for the above set of parameters, Fig. 1 shows that $\delta \sim 2$ is close to the minimum value of the perpendicular width. The velocity of the structure also appears to have a strong effect on the possible widths of electron holes.

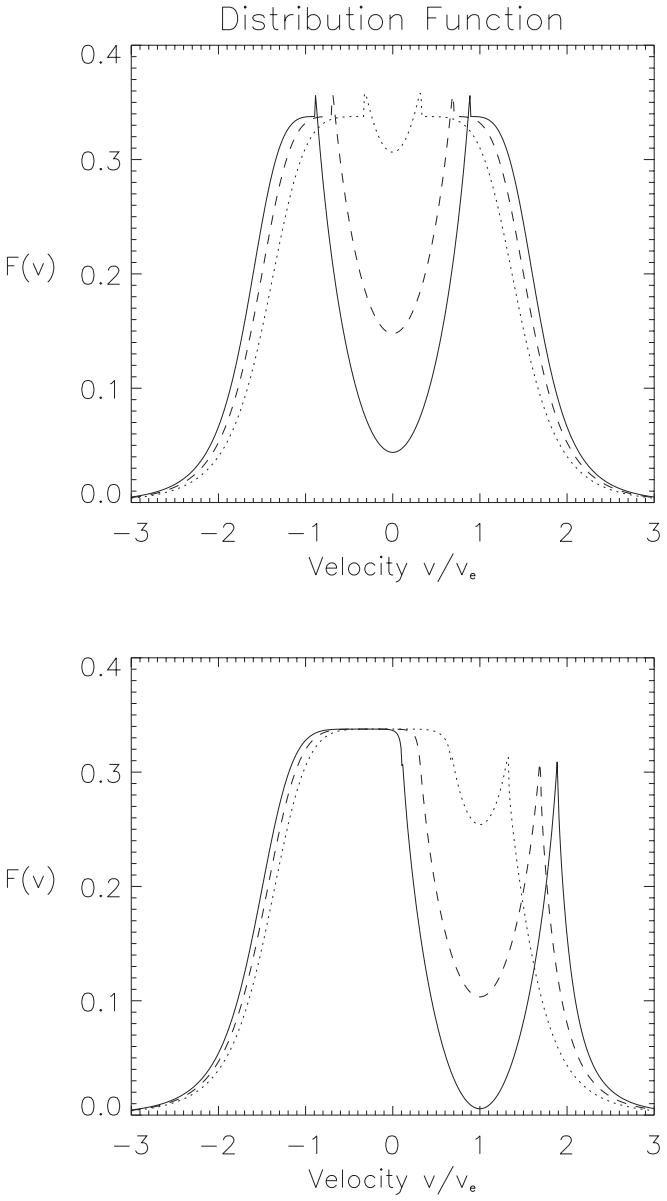

FIG. 1. 3D electron hole distribution function as a function of normalized velocity. The solid, dashed, and dotted lines correspond to $z=0$, $z=\Delta$, and $z=2\Delta$, respectively. A drift velocity $V=1$ is included in the lower panel. Hole parameters are $\Gamma=0.4$, $\Delta=2.6$, and $\delta=2$.

III. HAMILTONIAN FORMALISM FOR 3D ELECTRON HOLES

In this section, we introduce the Hamiltonian formalism of action-angle variables which is well-suited to the study of the dynamics of trapped electrons and of their interaction with electrostatic perturbations.[47] The Hamilton function of trapped electrons in Cartesian coordinates $(\vec{q},\vec{p})$ reads

$$H = \frac{1}{2m}(\vec{p} - e\vec{A})^2 - e\Phi_0(\vec{q}), \tag{11}$$

where $\vec{p}=m\vec{v}-e\vec{A}$ is the electron momentum, $\vec{q}=(x,y,z)$ and $\vec{A}$ is the vector potential which reduces to $\vec{A}=-eBy\vec{x}$ for the electrostatic case we study. In this form, H is not separable but by using successive generating functions, and it is possible to exhibit the different basic motions of trapped electrons and to find an approximate separable Hamiltonian for our problem. As a first step we use the generating function

$$F(\vec{q},\vec{Q}) = F[(x,y),(\varphi,Y)] = m\Omega_{ce}\left[\tfrac{1}{2}(y-Y)^2 \cot\varphi - xY\right]. \tag{12}$$

According to Hamiltonian theory,[48] $\vec{p}=\partial_{\vec{q}}F(\vec{q},\vec{Q})$ and $\vec{P}=-\partial_{\vec{Q}}F(\vec{q},\vec{Q})$ which gives the following relations among old $(\vec{q},\vec{p})$ and new $(\vec{Q},\vec{P})$ canonical variables

$$\tan\varphi = (p_x + eBy)/p_y, \tag{13}$$

$$Y = y + \rho_L \sin\varphi, \tag{14}$$

$$P_Y/(m\Omega_{ce}) = x - \rho_L \cos\varphi, \tag{15}$$

$$P_\varphi = mv_\perp^2/(2\Omega_{ce}). \tag{16}$$

We can interpret the new variables φ and Y as the gyrophase of the cyclotron motion and the ordinate of the gyrocenter position, respectively. The electron Larmor radius is $\rho_L = v_\perp/\Omega_{ce}$ and $X=P_Y/(m\Omega_{ce})$ can be interpreted as the abscissa of the gyrocenter. Since $F(\vec{q},\vec{Q})$ does not explicitly depend on time, the new Hamiltonian is the old one expressed as a function of the new variables, $H = P_z^2/2m + \Omega_{ce}P_\varphi - e\Phi_0(X+\rho_L\cos\varphi, Y-\rho_L\sin\varphi, z)$. As mentioned in Sec. II, in the strongly magnetized auroral plasma, we have $\rho_L \ll \Phi_0/\nabla_\perp\Phi_0 \sim \delta$, which means that we can develop to first order in ρ_L/δ the potential of the electron hole $\Phi_0 \sim \Phi_0(X,Y,z) + \vec{\rho_L}\cdot\vec{\nabla}\Phi_0(X,Y,z)$, where $\vec{\rho_L} = \rho_L(\cos\varphi, -\sin\varphi, 0)$. From Hamilton equations, we have $dP_\varphi/dt = -d\vec{\rho_L}/d\varphi\cdot\vec{\nabla}\Phi_0(X,Y,z)$ which averages out on a gyroperiod. According to Eq. (4), Ω_{ce}^{-1} is the fastest time scale of the problem and P_φ is therefore an adiabatic invariant, while the electron hole potential can be approximated by its gyro-average $\langle\Phi_0\rangle_\varphi \sim \Phi_0(X,Y,z)$. Due to the specific form of the potential given in Eq. (1), the Hamilton function reduces to

$$H = \frac{P_z^2}{2m} + \Omega_{ce}P_\varphi - e\Gamma a\left[\left(\frac{P_Y^2}{m^2\Omega_{ce}^2} + Y^2\right)^{1/2}\right]h(z). \tag{17}$$

This expression suggests using an harmonic oscillator type generating function $G(Y,\psi) = m\Omega_{ce}(\cot\psi)Y^2/2$ from which we obtain

$$Y = \sqrt{\frac{2P_\psi}{m\Omega_{ce}}}\sin\psi, \tag{18}$$

$$P_Y/(m\Omega_{ce}) = \sqrt{\frac{2P_\psi}{m\Omega_{ce}}}\cos\psi. \tag{19}$$

The new Hamilton function reads

$$H = \frac{P_z^2}{2m} + \Omega_{ce}P_\varphi - e\Gamma a\left[\left(\frac{2P_\psi}{m\Omega_{ce}}\right)^{1/2}\right]h(z). \tag{20}$$

Hamilton equations show that P_ψ is a constant of the motion which proves that the gyrocenter trajectory develops on a shell of constant radius $R=[2P_\psi/(m\Omega_{ce})]^{1/2}$. This shows the consistency of the approximations that we made in Sec. II.

From this point, it is straightforward to apply the Hamilton–Jacobi method in order to define three sets of action-angle variables: we just have to find a function $W[(z,\varphi,\psi),(P_Z,P_\Phi,P_\Psi)] = W_z(z,\vec{P}) + W_\varphi(\varphi,\vec{P}) + W_\psi(\psi,\vec{P})$ which satisfies the equation

$$\frac{(\partial_z W_z)^2}{2m} + \Omega_{ce}\partial_\varphi W_\varphi - e\Gamma a\left[\left(\frac{2\partial_\psi W_\psi}{m\Omega_{ce}}\right)^{1/2}\right]h(z) = E \tag{21}$$

with E as the energy of the trapped electron. We see that $W_\varphi=\varphi P_\Phi$ and $W_\psi=\psi P_\Psi$ are satisfying this equation if we take $P_\Phi=P_\varphi$ and $P_\Psi=P_\psi$ which are constant. The corresponding action variables are defined as

$$I_\Phi = \frac{1}{2\pi}\oint \partial_\varphi W_\varphi d\varphi = P_\Phi, \tag{22}$$

$$I_\Psi = \frac{1}{2\pi}\oint \partial_\psi W_\psi d\psi = P_\Psi, \tag{23}$$

$$I_z = \frac{1}{2\pi}\oint \partial_z W_z dz. \tag{24}$$

In addition we must find a function $W_z(z,\vec{P})$ which verifies the equation

$$\partial_z W_z = \pm\sqrt{2m\left\{E - \Omega_{ce}P_\Phi + e\Gamma a\left[\left(\frac{2P_\Psi}{m\Omega_{ce}}\right)^{1/2}\right]h(z)\right\}} = \pm\sqrt{f(z)}. \tag{25}$$

It is possible to integrate this equation numerically and we deduce from this expression the third action variable

$$I_z = \frac{1}{2\pi}\left\{\int_{-z_0}^{z_0}\sqrt{f(z)}dz + \int_{z_0}^{-z_0}[-\sqrt{f(z)}]dz\right\}, \tag{26}$$

where the cyclic integral has two contributions since trapped electrons bounce back and forth along the $\vec{z}$ direction with turning points z_0 defined by the relation $f(z_0)=0$. We can write I_z as

$$I_z = \frac{2\Delta\sqrt{-2mE_\parallel}}{\pi} K\left(\left\{-2\ln\left[\frac{-E_\parallel}{e\Gamma a(R)}\right]\right\}^{1/2}\right) \tag{27}$$

with $K(u_0)=\int_0^{u_0}\sqrt{-1+\exp[(u_0^2-u^2)/2]}du$ and $E_\parallel = E-\Omega_{ce}P_\Phi$ is the parallel energy as defined in Sec. II. This clearly shows that I_z is a function of $E_\parallel$ and R. This relation can be inverted and $E_\parallel$ can be considered as a function of I_z and I_Ψ since R is a function of I_Ψ. Finally, we have found the unperturbed Hamiltonian of our problem

$$H_0(\vec{I}) = E_\parallel(I_z, I_\Psi) + \Omega_{ce} I_\Phi. \tag{28}$$

The corresponding action-angle variables $\vec{I}=(I_z, I_\Phi, I_\Psi)$ and $\vec{\theta}=(\theta_z, \Phi, \Psi)$ satisfy Hamilton equations

$$\frac{d}{dt}\vec{I} = -\frac{\partial H_0}{\partial \vec{\theta}}, \tag{29}$$

$$\frac{d}{dt}\vec{\theta} = +\frac{\partial H_0}{\partial \vec{I}}, \tag{30}$$

which implies that $\vec{I}$ is constant and that $\vec{\theta}=\vec{\Omega}t+\vec{\theta}_0$, where $\vec{\Omega}=\partial_{\vec{I}}H_0$ is also a constant vector. This vector can be written as

$$\vec{\Omega} = [\omega_b(I_z, I_\Psi), \Omega_{ce}(I_\Phi), \omega_\gamma(I_z, I_\Psi)], \tag{31}$$

where ω_b and ω_γ are the bounce and drift pulsations that were introduced in Sec. II. After one cycle in $(\vec{q},\vec{p})$ coordinates, angle variables changed by $\Delta\theta_j = \oint \partial_{q_j}\theta_j \cdot dq_i$. If we now define the generatrice function $W'(\vec{q},\vec{I})$ such that $\vec{\theta} = \partial_{\vec{I}}W'$ and $\vec{p}=\partial_{\vec{q}}W'$, we see that $\Delta\theta_j = \oint \partial^2_{q_i I_j} W' dq_i = \partial_{I_j}\oint \vec{p}\cdot d\vec{q} = 2\pi\delta_{ij}$. This shows that θ_j is an angle variable that increases by 2π after each cycle of the (x_i, p_i) coordinate.

IV. PERTURBATION OF THE 3D EQUILIBRIUM

Let us now perturb this Hamiltonian system with a monochromatic electrostatic wave defined by

$$\delta\Phi(y,z,t) = \mathrm{Re}\{\delta\Phi_0 \exp[i(k_\parallel z + k_\perp y - \omega t)]\}, \tag{32}$$

where Re{.} stands for the real part, $\vec{k}=k_\parallel\vec{z}+k_\perp\vec{y}$ is the wave vector, and ω its pulsation. The wave amplitude is assumed to be small compared to the electron hole amplitude Γ and we define a small parameter $\varepsilon = -e\delta\Phi_0/\Gamma$. When this perturbation is switched on, we can define a new Hamilton function

$$H(\vec{I},\vec{\theta},t) = H_0(\vec{I}) + \varepsilon\Psi(\vec{I},\vec{\theta},t), \tag{33}$$

where $\delta\Phi(y,z,t)$ transformed into $\Psi(\vec{I},\vec{\theta},t)$ since any function of $(\vec{q},\vec{p})$ is a function of $(\vec{I},\vec{\theta})$. We know that $\Psi(\vec{I},\vec{\theta},t)$, which is a periodic function in each θ_i, can be developed in a Fourier series in $\vec{\theta}$ of the form

$$\Psi(\vec{I},\vec{\theta},t) = \mathrm{Re}\left\{\sum_{\vec{K}\in\mathbb{Z}^3} a_{\vec{K}}(\vec{I})\exp[i(\vec{K}\cdot\vec{\theta}-\omega t)]\right\}, \tag{34}$$

where $\vec{K}=(K_z, K_\Phi, K_\Psi)$ is a triplet of integer numbers. Provided that the wavelength of the perturbation is larger than the electron Larmor radius ($\lambda \gg \rho_L$), we can neglect the small-scale electron gyromotion which means that the only nonvanishing terms of the development will have $K_\Phi=0$. This assumption, that is critical for our derivation, is satisfied for electrostatic whistler waves in the strongly magnetized auroral plasma since the electron Debye length is larger than the electron Larmor radius and since sub-Debye length electrostatic whistler waves are strongly Landau damped. This reduces the summation over $\vec{K}\in\mathbb{Z}^2$. Using a quadratic approximation for the parallel motion in the potential well of the electron hole, we have $\Phi_0(R,z)\sim\Gamma(1-z^2/2\Delta^2)a(R)$ and the parallel trajectory reduces to $z=\alpha\sin\theta_z$ with $\alpha = \sqrt{2\Delta^2[E_\parallel/[e\Gamma a(R)]+1]}$. According to Sec. III, the coordinates of the electron gyrocenter are $(R\cos\Psi, R\sin\Psi)$. Introducing Bessel functions J_n which satisfy the relation $\exp(i\alpha\sin\varphi)=\sum_{p=-\infty}^{\infty}J_p(\alpha)\exp(ip\varphi)$ we obtain

$$c_{\vec{K}} = \varepsilon a_{\vec{K}}(\vec{I}) = -e\delta\Phi_0 J_{K_z}(k_z\alpha)J_{K_\Psi}(k_y R). \tag{35}$$

The perturbation distorts electron trajectories and action-angle variables for perturbed trapped electrons can be expanded in a power series in ε around their undisturbed value $[\vec{I}^{(0)},\vec{\theta}^{(0)}]$ according to

$$\begin{aligned}\vec{I} &= \vec{I}^{(0)} + \varepsilon\vec{I}^{(1)} + \varepsilon^2\vec{I}^{(2)} + \cdots,\\ \vec{\theta} &= \vec{\theta}^{(0)} + \varepsilon\vec{\theta}^{(1)} + \varepsilon^2\vec{\theta}^{(2)} + \cdots.\end{aligned} \tag{36}$$

We aim at evaluating the amount of energy gained or lost after some time t by an electron $\Delta E[\vec{I}^{(0)},\vec{\theta}^{(0)},t]$ whose initial position in phase space is defined by $\vec{I}^{(0)}$ and $\vec{\theta}^{(0)}$. Under the linearity condition, we assume that over this time t the amplitude of the electron hole Γ does not vary. The Taylor expansion of H_0 around $\vec{I}^{(0)}$ to second order in ε leads to

$$\begin{aligned}\Delta E[\vec{I}^{(0)},\vec{\theta}^{(0)},t] &= \Delta[H_0(\vec{I})]\\ &\sim \varepsilon\vec{\Omega}\cdot\vec{I}^{(1)} + \varepsilon^2\left\{\vec{\Omega}\cdot\vec{I}^{(2)} + \tfrac{1}{2}\vec{I}^{(1)}\cdot[\partial_{\vec{I}}\vec{\Omega}:\vec{I}^{(1)}]\right\},\end{aligned} \tag{37}$$

where the symbol ":" holds for dyadic contraction.

Perturbed action-angle variables have to satisfy Hamilton equations and we need to solve them order by order in ε. At first order in ε, this yields

$$\frac{d}{dt}\vec{I}^{(1)} = -\partial_{\vec{\theta}}\Psi|_0, \tag{38}$$

$$\frac{d}{dt}\vec{\theta}^{(1)} = \partial^2_{\vec{I}^2}H_0|_0 : \vec{I}^{(1)} + \partial_{\vec{I}}\Psi|_0, \tag{39}$$

where the subscript $|0$ means that derivatives are taken along the undisturbed phase space trajectory $[\vec{I}^{(0)},\vec{\theta}^{(0)}]$. Using the definition $\vec{\Omega}=\partial_{\vec{I}}H_0$ and after time integration we obtain

$$\vec{I}^{(1)}=-\mathrm{Re}\left\{\sum_{\vec{K}\in\mathbb{Z}^2}\exp[i\vec{K}\cdot\vec{\theta}^{(0)}]\vec{K}a_{\vec{K}}[\vec{I}^{(0)}]\frac{\exp(i\omega_{\vec{K}}t)-1}{\omega_{\vec{K}}}\right\}, \tag{40}$$

$$\vec{\theta}^{(1)}=-\mathrm{Re}\left\{\sum_{\vec{K}\in\mathbb{Z}^2}\exp[i\vec{K}\cdot\vec{\theta}^{(0)}]\times\left\{\partial^2_{\vec{I}^2}H_0|_0\vec{K}a_{\vec{K}}[\vec{I}^{(0)}]\frac{\exp(i\omega_{\vec{K}}t)-1-\omega_{\vec{K}}t}{i\omega^2_{\vec{K}}}-\partial_{\vec{I}}a_{\vec{K}}|_0\frac{\exp(i\omega_{\vec{K}}t)-1}{i\omega_{\vec{K}}}\right]\right\}, \tag{41}$$

where $\omega_{\vec{K}}=\vec{K}\cdot\vec{\Omega}[\vec{I}^{(0)}]-\omega$ is a quantity that can potentially vanish for specific sets of action variables. In such a case both $\vec{I}^{(1)}$ and $\vec{\theta}^{(1)}$ become resonant whereby the energy gain or loss by the trapped electron with a given initial phase space position will be important. This resonant condition is a generalization in 3D of the bounce resonance that was identified in the 1D case.[47,49] In 3D it involves the three characteristic frequencies of the electron motion. At this time, it is important to notice that the average over initial angle variables of $\vec{I}^{(1)}$ would be

$$\langle\vec{I}^{(1)}\rangle_{\vec{\theta}^{(0)}}=0. \tag{42}$$

At second order in ε, the Hamilton equation for $\vec{I}^{(2)}$ gives

$$\frac{d}{dt}\vec{I}^{(2)}=-\partial^2_{\vec{I}\vec{\theta}}\Psi|_0:\vec{I}^{(1)}-\partial^2_{\vec{\theta}^2}\Psi|_0:\vec{\theta}^{(1)}. \tag{43}$$

If we only keep resonant terms when performing time integration, one can show after some lengthy calculations that the average over $\vec{\theta}^{(0)}$ of $\vec{I}^{(2)}$ reduces to

$$\langle\vec{I}^{(2)}\rangle_{\vec{\theta}^{(0)}}=t^3\sum_{\vec{K}\in\mathbb{Z}^2}\vec{K}|a_{\vec{K}}|^2\vec{K}\cdot(\partial^2_{\vec{I}^2}H_0|_0:\vec{K})g(\omega_{\vec{K}}t), \tag{44}$$

where $g(u)=[2(\cos u-1)/u^2+\sin u/u]/(2u)$. We conclude that the average energy exchanged between trapped particles and the perturbation is

$$\langle\Delta E\rangle_{\vec{\theta}^{(0)}}=\varepsilon^2\left\{\vec{\Omega}\cdot\langle\vec{I}^{(2)}\rangle_{\vec{\theta}^{(0)}}+\frac{1}{2}\langle\vec{I}^{(1)}\cdot[\partial_{\vec{I}}\vec{\Omega}:\vec{I}^{(1)}]\rangle_{\vec{\theta}^{(0)}}\right\} \tag{45}$$

since at first order there is no average energy exchanged. Hereafter we only consider the first term of Eq. (45) which is dominant since it is proportional to $\omega_{\vec{K}}^{-3}$ while the second one varies as $\omega_{\vec{K}}^{-2}$. It can be shown that for that reason the second term does not survive the next step of calculation. Combining Eqs. (40) and (44) with Eq. (45), we finally get

$$\langle\Delta E\rangle_{\vec{\theta}^{(0)}}=t^3\sum_{\vec{K}\in\mathbb{Z}^2}|c_{\vec{K}}|^2(\partial^2_{\vec{I}^2}H_0|_0:\vec{K})(\vec{\Omega}\cdot\vec{K})g(\omega_{\vec{K}}t) \tag{46}$$

which is a function of $\vec{I}_\parallel=(I_z,I_\Psi)$ only since $\partial^2_{\vec{I}I_\Phi}H_0=\vec{0}$.

V. GROWTH RATE OF ELECTROSTATIC WAVES

We consider that the distribution function of trapped electrons f_t is not affected by the resonant process over the time scale of the linear instability. It allows us to average over phase space the energy given by the perturbation to the trapped particles as

$$\langle\Delta E\rangle=\int_{E_\parallel<0}f_t(\vec{p},\vec{q})\Delta E(\vec{p},\vec{q})d\vec{p}d\vec{q}. \tag{47}$$

In this integral, we weight the energy exchanged by one particle with the perturbation by the value of the distribution function at the initial phase space position of the particle. Since we have shown in Sec. III that P_Φ (or equivalently ρ_L) is constant and in Sec. II that f_t is cylindrically symmetric, we can write

$$f_t=\frac{1}{(2\pi)^2}f_t(R,z,p_z)\frac{\delta(v_\perp-\rho_L\Omega_{ce})}{v_\perp}, \tag{48}$$

where $\delta(.)$ is the Dirac distribution. It is also convenient to make the change of variable from p_z to $E_\parallel$ since we know that the trapped distribution only depends on $E_\parallel$ and R. We notice that the integration over the initial position z is equivalent to an integration over the corresponding angle variable θ_z which implies that $\oint dz/v_z$ is equivalent to $1/\omega_b(R,E_\parallel)\int_0^{2\pi}d\theta_z$. Finally, we change from $(R,E_\parallel)$ variables to $\vec{I}_\parallel$ action variables and we get

$$\langle\Delta E\rangle=\frac{\pi}{m}\int\int\langle\Delta E\rangle_{\vec{\theta}^{(0)}}\frac{f_t(\vec{I}_\parallel)R(\vec{I}_\parallel)}{\omega_b(\vec{I}_\parallel)}J(\vec{I}_\parallel)d\vec{I}_\parallel, \tag{49}$$

where $J(\vec{I}_\parallel)=\omega_b(\vec{I}_\parallel)/[R(\vec{I}_\parallel)\Omega_{ce}]$ is the Jacobian function of the last transformation.

Since the integrand is resonant around the 2D curve D_{res} defined by the resonance condition $\omega_{\vec{K}}(\vec{I}_{\parallel\mathrm{res}})=0$, we can expand $f_t(\vec{I}_\parallel)$ around the resonant action $\vec{I}_{\parallel\mathrm{res}}$,

$$f_t(\vec{I}_\parallel)\sim f_t(\vec{I}_{\parallel\mathrm{res}})+(\vec{I}_\parallel-\vec{I}_{\parallel\mathrm{res}})\cdot\partial_{\vec{I}_\parallel}f_t|_{\mathrm{res}}+\ldots, \tag{50}$$

where the subscript $|\mathrm{res}$ means that the derivative is taken at the resonance point. In order to evaluate this 2D integral, we consider a new reference frame with axis along and across the resonant curve such that any vector can be written as $\vec{I}_\parallel=\vec{I}_{\parallel\mathrm{res}}+x\vec{N}$ with $\vec{I}_{\parallel\mathrm{res}}\cdot\vec{N}=0$. The Jacobian of this isometric transformation is unity. In this frame, $f_t(\vec{I}_\parallel)=f_t(\vec{I}_{\parallel\mathrm{res}})+x\vec{N}\cdot\partial_{\vec{I}_\parallel}f_t|_{\mathrm{res}}$ and $\omega_{\vec{K}}=x\vec{N}\cdot\partial_{\vec{I}_\parallel}(\vec{\Omega}\cdot\vec{K})|_{\mathrm{res}}$ and we obtain

$$\langle\Delta E\rangle=\frac{\pi t^3}{m\Omega_{ce}}\int_{D_{\mathrm{res}}}|c_{\vec{K}}|^2(\vec{I}_{\parallel\mathrm{res}})\vec{K}\cdot(\partial^2_{\vec{I}^2}H_0|_{\mathrm{res}}:\vec{K})S(\vec{I}_{\parallel\mathrm{res}})dI_{\parallel\mathrm{res}} \tag{51}$$

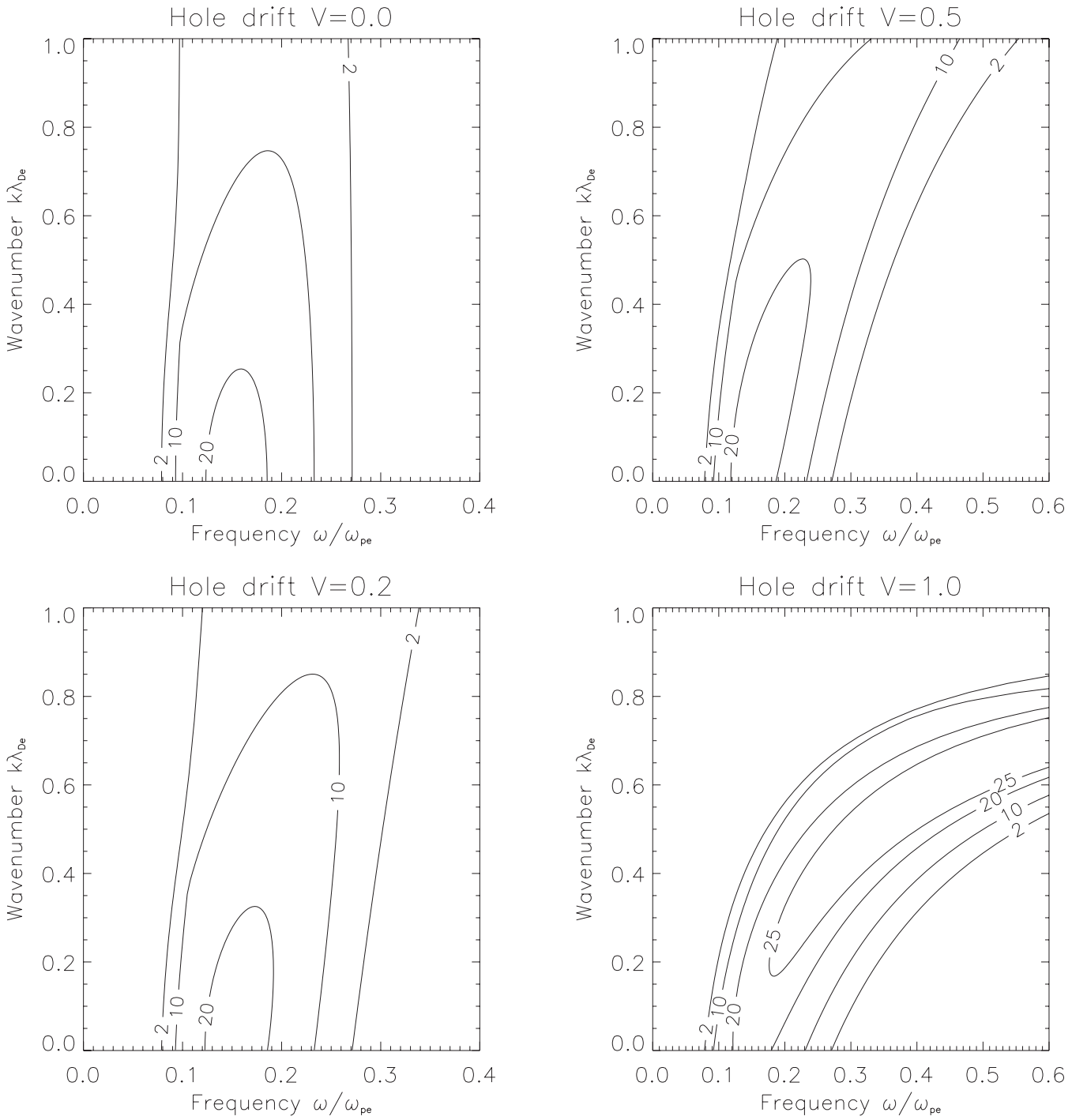

FIG. 2. Growth rate in percent of the wave frequency vs normalized wave number and frequency for drift velocity $V=0$, $V=0.2$, $V=0.5$, and $V=1$. Other parameters are $\Omega_{ce}/\omega_{pe}=5$, $\Gamma=0.35$, $\Delta=2$, and $\delta=2$. Landau damping is not included.

with

$$S(\vec{I}_{\|\mathrm{res}}) = \int_{-\infty}^{+\infty} [\omega + x\vec{N}\cdot\partial_{\vec{I}_{\|}}(\vec{\Omega}\cdot\vec{K})|_{\mathrm{res}}]g[x\vec{N}\cdot\partial_{\vec{I}_{\|}}(\vec{\Omega}\cdot\vec{K})|_{\mathrm{res}}t] \times [f_t(\vec{I}_{\|\mathrm{res}}) + x\vec{N}\cdot\partial_{\vec{I}_{\|}} f_t|_{\mathrm{res}}]dx. \quad (52)$$

Some simplifications can be made due to the parity of the integrand terms and we get

$$S(\vec{I}_{\|\mathrm{res}}) = -\frac{\pi\omega\vec{N}\cdot\partial_{\vec{I}_{\|}} f_t|_{\mathrm{res}}}{t^2 2[\partial_{\vec{I}_{\|}}(\vec{\Omega}\cdot\vec{K})|_{\mathrm{res}}]^2}. \quad (53)$$

This shows that $\langle\Delta E\rangle \propto t$. This secular variation results from the 3D resonant interaction of trapped particles with the wave. Let us now define V_{hole} as the electron hole volume. Then the energy exchanged by one electron hole with the wave after time t is given by the quantity $\delta E_t(t) = \langle\Delta E\rangle n_e V_{\mathrm{hole}}$, where n_e is the unperturbed electron density.

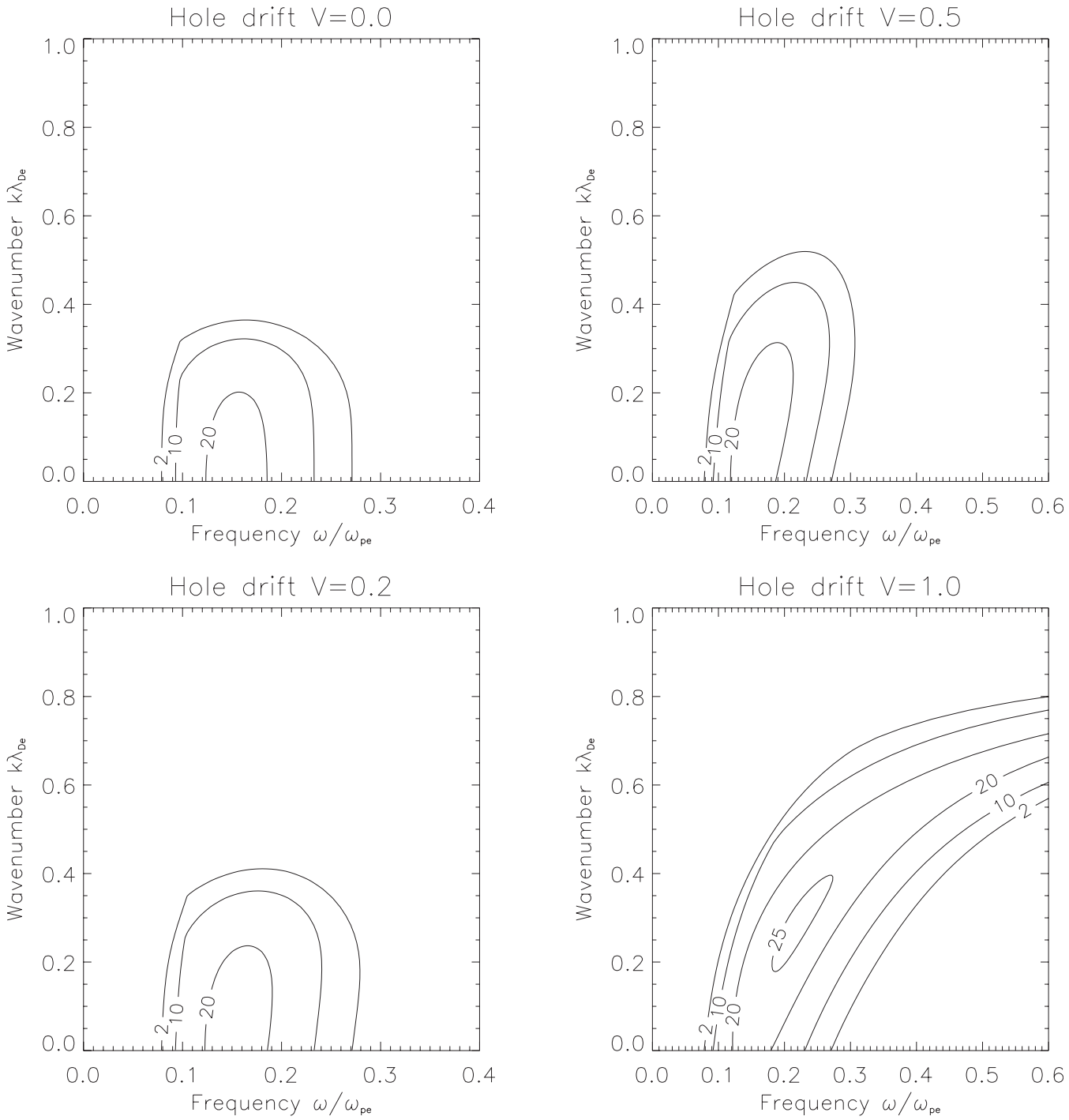

FIG. 3. Same as Fig. 2 but with Landau damping included.

We define a repetition parameter L as the ratio between the averaged distance between two electron holes and the averaged size of individual electron holes along a given dimension of space. The quantity $E_W L^3 V_{\text{hole}}$ is therefore the averaged wave energy that should be compared with $\delta E_t(t)$. The wave energy density is defined as $E_W=\varepsilon_0 k^2|\delta\Phi_0|^2/2$ and defining its complex frequency as $\omega+i\gamma$, we conclude from energy conservation that $\delta E_t(t)/t=-2\gamma E_W L^3 V_{\text{hole}}$ which finally gives the normalized growth rate of the perturbation as $\gamma/\omega=-n_e V_{\text{hole}}\langle\Delta E\rangle/[2\omega t E_W L^3 V_{\text{hole}}]$. Using the normalizations of Sec. II, we eventually obtained the expression

$$\frac{\gamma}{\omega}=\frac{\pi^2}{2(\Omega_{ce}/\omega_{pe})k^2L^3}\times\sum_{\vec{K}\in\mathbb{Z}^2}\int_{D_{\text{res}}}\frac{J^2_{K_z}(k_\parallel\alpha_{\text{res}})J^2_{K_\Psi}(k_\perp R_{\text{res}})\vec{K}\cdot(\partial^2_{\vec{I}^2}H_0|_{\text{res}}:\vec{K})}{[\partial_{\vec{I}_\parallel}(\vec{\Omega}\cdot\vec{K})|_{\text{res}}]^2}\times\vec{N}\cdot\partial_{\vec{I}_\parallel}f_t|_{\text{res}}dI_{\parallel\text{res}}. \quad (54)$$

It must be mentioned that standard Landau damping from passing particles interacting with the perturbation gives an

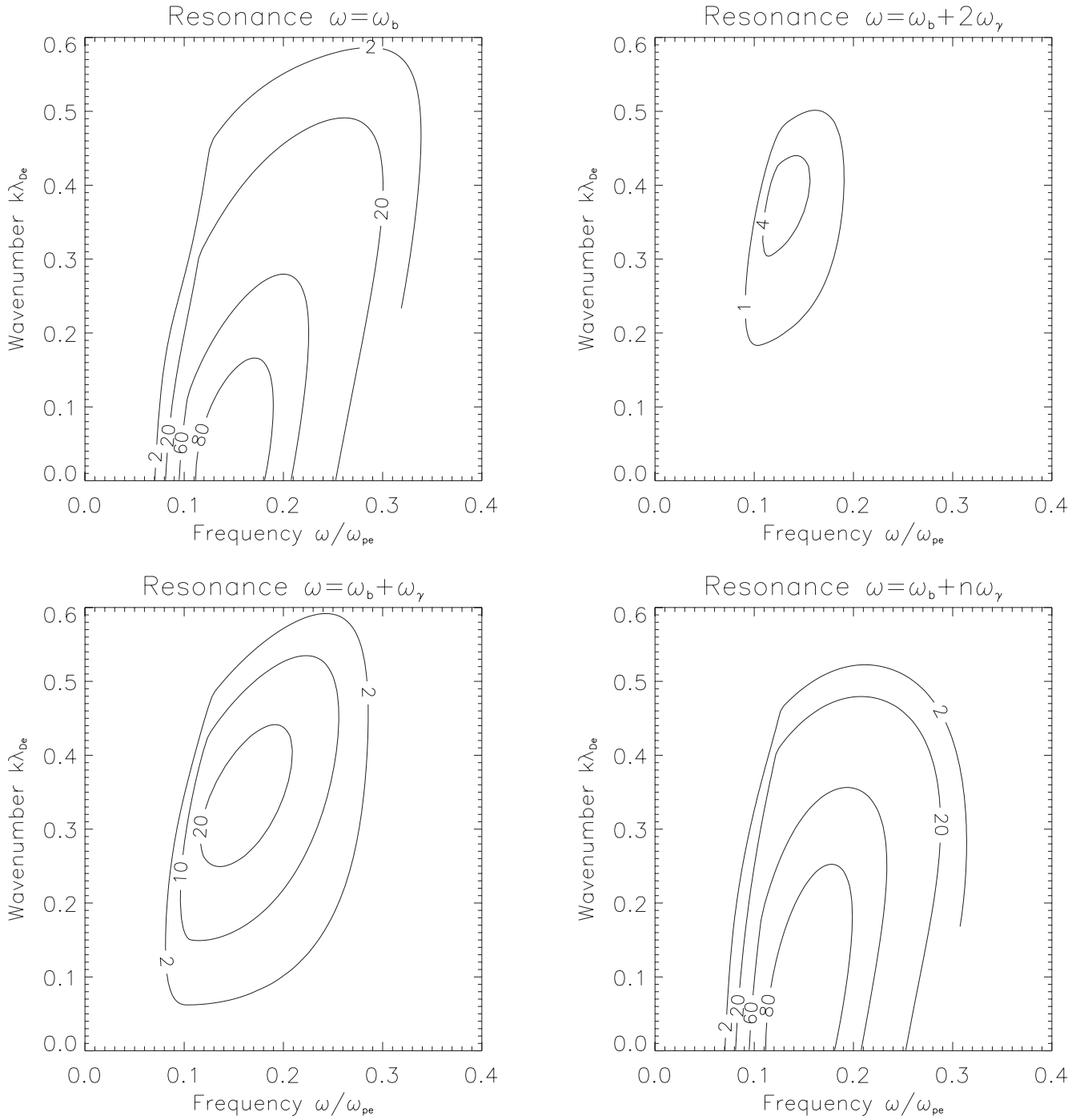

FIG. 4. Same format as Fig. 2. Different resonance conditions are considered. Parameters are $\Omega_{ce}/\omega_{pe}=5$, $\Gamma=0.35$, $\Delta=2$, $\delta=4$, and $V=0.5$.

additional term to this equation of the form $\gamma_L/\omega = \pi/(2k^2)\,(df_p/dv_\parallel)|_{\omega/k_\parallel}$.

VI. NUMERICAL RESULTS

From this point, it is possible to compute this growth rate for different plasma, wave, and electron hole parameters and to look at the regions in parameter space where the growth rate is large and positive, i.e., where the 3D electron hole can be destabilized by its interaction with electrostatic whistler wave (EWW) perturbations. Figure 2 displays the contour plot of the growth rate γ, which is given in percents of the wave frequency ω, as a function of the wave frequency (normalized to ω_{pe}) and of the wavenumber (normalized to λ_{De}^{-1}). Here we only take into account the growth rate due to the trapped particles. Parameters have been chosen such that $\Omega_{ce}/\omega_{pe}=5$, $\Gamma=0.35$, $\Delta=2$, $\delta=2$, $K_z=1$, and $K_\Psi=0$ while the electron hole drift V relative to the passing electrons distribution function varies between 0 and 1 in the four panels. Similarly to the 1D case, the emission process is efficient over a wide range of frequencies and wavenumbers. The actual values of the growth rate strongly depend on the repetition parameter that we fixed hereafter at $L=3$. As long as $L \lesssim 10$, we obtain significant growth rates for this linear

instability. When the electron hole drift increases, the contour plots stretch towards higher frequencies due to the Doppler effect and the maximum growth rate increases. Figure 3 includes the effect of Landau damping. The main effect of Landau damping is to confine EWW emission to low (below λ_{De}^{-1}) wavenumbers. However Landau damping does not significantly reduce the maximum growth rate. In the following figures we always included Landau damping.

Figure 4 shows the relative contribution to the growth rate of the first terms of the sum over $\vec{K}$ in Eq. (54). Here $\Omega_{ce}/\omega_{pe}=5$, $\Gamma=0.35$, $\Delta=2$, $\delta=4$, and $V=0.5$. As a reference, the left upper panel corresponds to the resonance condition $\omega=\omega_b$ while the effect of the first and second harmonics of the drift frequency ω_γ is shown in the other panels. In the right lower panel we performed the summation over all values of K_Ψ. We see that higher harmonics only contribute to small wavelength emissions. The growth rate also strongly decreases with increasing values of K_Ψ. This is due to the Bessel term $J_{K_\Psi}^2(k_\perp R_{\rm res})$ which vanishes as soon as $K_\Psi \gtrsim k_\perp R_{\rm res}$. A detailed study of the resonance curve $D_{\rm res}$ shows that $R_{\rm res}$ is always of the order of δ which is the perpendicular width of the structure. Therefore we only need to consider $K_\Psi \lesssim k_\perp \delta$, i.e., $K_\Psi \lesssim \delta$.

Figure 5 gives the contribution to the growth rate from the second harmonics of the bounce (upper panel) and the drift frequency (lower panel), respectively. Plasma and electron hole parameters are unchanged from Fig. 3. Note that the scale of the frequency axis varies from one plot to the other by one order of magnitude since $\omega_b \gg \omega_\gamma$. It is interesting to notice that the maximum (normalized) growth rate is given by the second harmonics of the drift frequency. However typical values of these growth rates are relatively weak. With the chosen parameters, the first harmonic of the drift frequency cannot match the frequency of the EWW since it is below the lower-hybrid frequency, which is the cutoff of this wave mode.

Figure 6 shows the effect of varying plasma magnetization from $\Omega_{ce}/\omega_{pe}=2$ (left panels) to $\Omega_{ce}/\omega_{pe}=20$ (right panels) and the parallel width of the electron hole from $\Delta=1.6$ (upper panels)—which is close to its minimum value for $\Gamma=0.35$, $\delta=4$, and $V=0.5$—to $\Delta=4$ (lower panels). Here we only consider the resonance at the bounce frequency. It is observed that plasma magnetization only slightly decreases the maximum growth rate of EWW. We also notice that wider structures along the magnetic field, which correspond to smaller bounce frequencies, excite lower frequency waves, down to the lower-hybrid frequency. The comparison of Figs. 5 and 6 shows that the emission of lower-hybrid waves by bounce resonance is more favorable than the emission by drift resonance.

Figure 7 shows how important δ is, the perpendicular width of the electron hole, for the emission of EWW by bounce resonance ($K_z=1$, $K_\Psi=0$). Plasma and hole parameters are $\Omega_{ce}/\omega_{pe}=10$, $\Gamma=0.2$, $\Delta=2$, and $V=0.5$ in this figure while δ is varying from 1 to 10. It is clear that the maximum growth rate strongly increases with δ and that the domain of instability of EWW simultaneously spreads in frequency and wavenumber space. The large growth rate values mean that

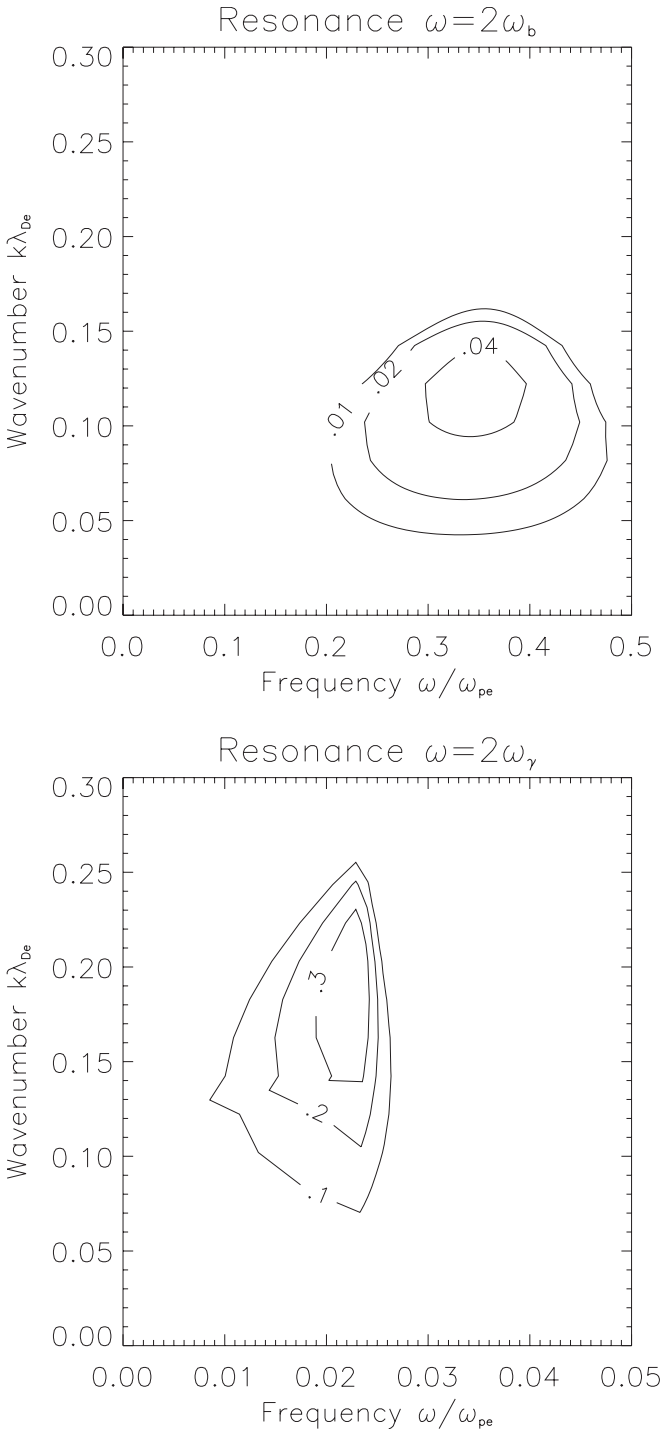

FIG. 5. Same format as Fig. 2. Resonance at the second harmonics of the bounce and drift frequency. Parameters are $\Omega_{ce}/\omega_{pe}=5$, $\Gamma=0.35$, $\Delta=2$, $\delta=2$, and $V=0.5$.

structures which are elongated across the magnetic field are highly unstable to the bounce resonance instability. However remember that the actual values of the growth rate directly depend on the repetition parameter of the electron holes L since $\gamma/\omega L^{-3}$. As a consequence of these large growth rates, we observed that the convection length of the bounce instability strongly decreases with increasing ratio δ/Δ. This means that EWW can be emitted from elongated electron

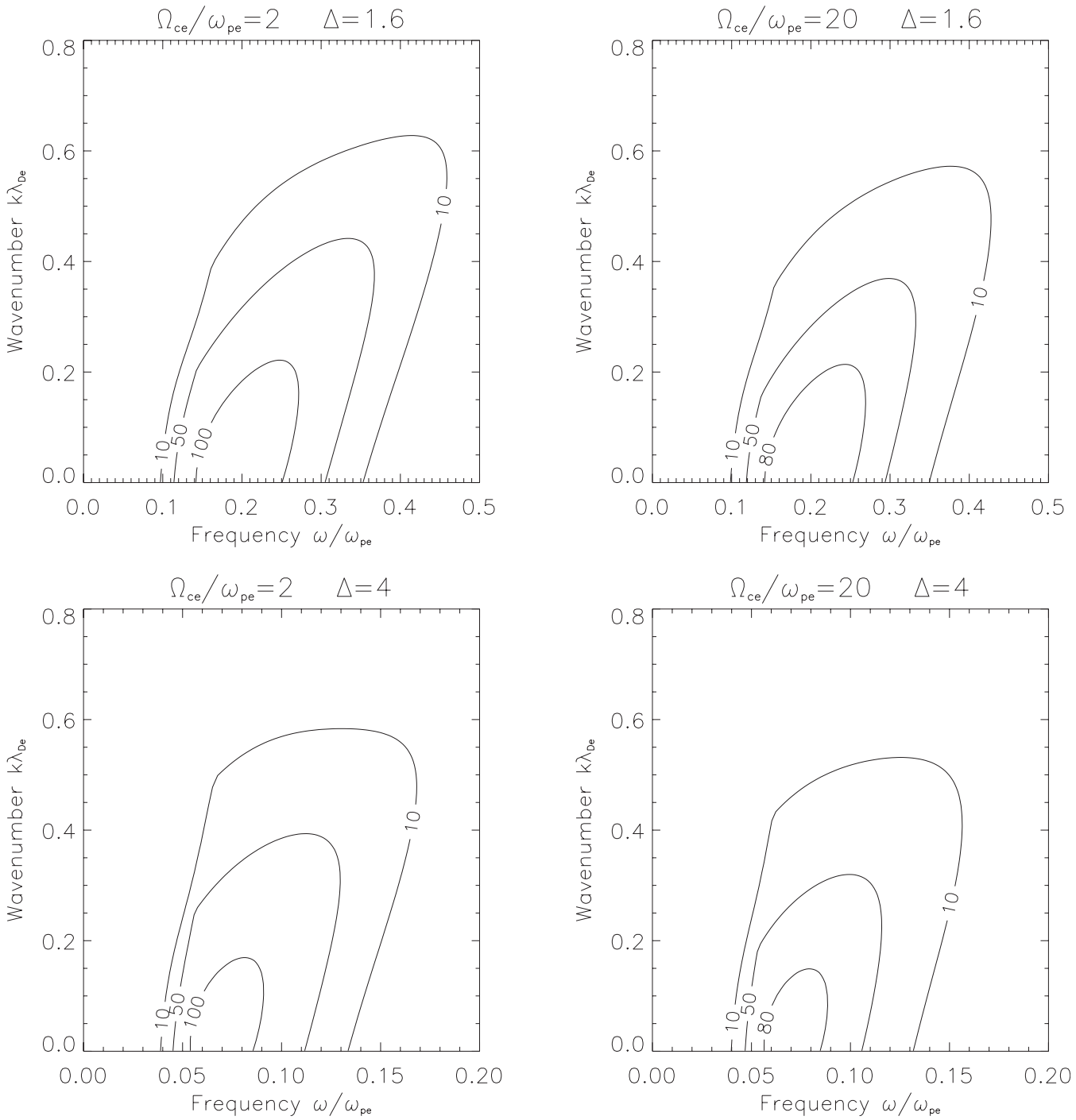

FIG. 6. Same format as Fig. 2. Plasma magnetization Ω_{ce}/ω_{pe} and parallel width of the electron hole Δ varies. Other parameters are $\Gamma=0.35$, $\delta=4$, and $V=0.5$.

holes within a few tens of Debye lengths or equivalently within a few kilometers in the auroral region. This process might therefore explain the emission of EWW in the form of VLF saucers. In order to further quantitatively compare these theoretical predictions with experimental data, it would be necessary to study the saturation mechanism of this instability.

VII. CONCLUSIONS

We have performed a detailed theoretical study of the stability of three-dimensional electron holes in a strongly magnetized plasma. We have first derived the exact distribution function of 3D drifting electron holes. We have shown that the amplitude-minimum width relationship of electron

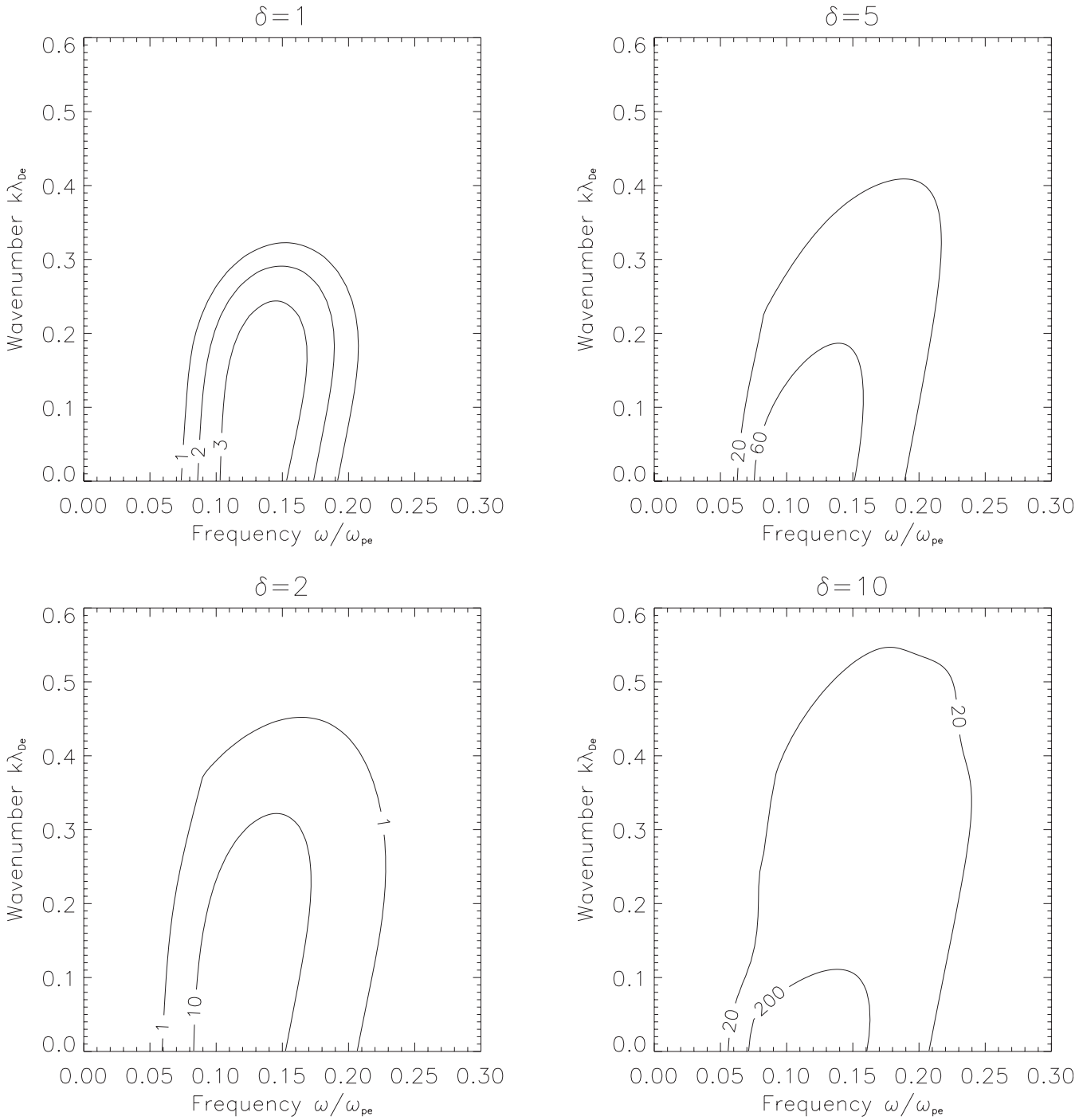

FIG. 7. Same format as Fig. 2. The perpendicular elongation of this electron hole δ varies. Other parameters are $\Omega_{ce}/\omega_{pe}=10$, $\Gamma=0.2$, $\Delta=2$, and $V=0.5$.

holes is strongly affected by the electron hole velocity relative to the passing particles. Introducing Hamiltonian formalism, we have defined a set of action-angle variables which allowed us to study the 3D dynamics of trapped particles. Canonical perturbation theory led to an estimate of the energy gained or lost by trapped electrons in their interaction with EWW. We have identified a generalized resonance condition which implies the bounce frequency along the magnetic field and the drift frequency across the magnetic field due to the "$\mathbf{E}\times\mathbf{B}$" drift associated with the electric field structure. An estimate of the growth rate of this linear instability has been derived by a complex averaging process. This general result does not depend on the particular choice of the passing distribution function.

The numerical study showed that the emission of EWW by bounce resonance is dominant. It can excite waves over a large frequency range, virtually from the lower-hybrid frequency cutoff up to the electron plasma frequency, depending mainly on the parallel width of the structure and on the electron hole drift relative to the passing electron frame. The strongest emissions have been found to occur for elongated structures across the magnetic field. A possible explanation of the production of VLF saucers by this process has been pointed out.

[1]C. W. Carlson, J. P. McFadden, R. E. Ergun, M. Temerin, W. Peria, F. S. Mozer, D. M. Klumpar, E. G. Shelley, W. K. Peterson, E. Moebius, R. Elphic, R. Strangeway, C. Cattell, and R. F. Pfaff, Geophys. Res. Lett. **25**, 2017, DOI:10.1029/98GL00851 (1998).
[2]R. E. Ergun, C. W. Carlson, J. P. McFadden, F. S. Mozer, G. T. Delory, W. Peria, C. C. Chaston, M. Temerin, I. Roth, L. Muschietti, R. Elphic, R. Strangeway, R. Pfaff, C. A. Cattell, D. Klumpar, E. Shelley, W. Peterson, E. Moebius, and L. Kistler, Geophys. Res. Lett. **25**, 2041, DOI:10.1029/98GL00636 (1998).
[3]H. Matsumoto, H. Kojima, T. Miyatake, Y. Omura, I. Nagano, and M. Tsutsui, Geophys. Res. Lett. **21**, 2915, DOI:10.1029/94GL01284 (1994).
[4]S. D. Bale, P. J. Kellogg, D. E. Larson, R. P. Lin, K. Goetz, and R. P. Lepping, Geophys. Res. Lett. **25**, 2929, DOI:10.1029/98GL02111 (1998).
[5]C. Cattell, C. Neiman, J. Dombeck, J. Crumley, J. Wygant, C. A. Kletzing, W. K. Peterson, F. S. Mozer, and M. André, Nonlinear Processes Geophys. **10**, 13 (2003).
[6]M. Temerin, K. Cerny, W. Lotko, and F. S. Mozer, Phys. Rev. Lett. **48**, 1175 (1982).
[7]M. Berthomier, R. Pottelette, and M. Malingre, J. Geophys. Res. **103**, 4261, DOI:10.1029/97JA00338 (1998).
[8]F. S. Mozer, R. E. Ergun, M. Temerin, C. Cattell, J. Dombeck, and J. Wygant, Phys. Rev. Lett. **79**, 1281 (1997).
[9]C. A. Cattell, J. Dombeck, J. R. Wygant, M. K. Hudson, F. S. Mozer, M. A. Temerin, W. K. Peterson, C. A. Kletzing, C. T. Russell, and R. F. Pfaff, Geophys. Res. Lett. **26**, 425, DOI:10.1029/1998GL900304 (1999).
[10]J. R. Franz, P. M. Kintner, C. E. Seyler, J. S. Pickett, and J. D. Scudder, Geophys. Res. Lett. **27**, 169, DOI:10.1029/1999GL010733 (2000).
[11]R. L. Tokar and S. P. Gary, Geophys. Res. Lett. **11**, 1180, DOI:10.1029/GL011i012p01180 (1984).
[12]N. Dubouloz, R. Pottelette, M. Malingre, and R. A. Treumann, Geophys. Res. Lett. **18**, 155, DOI:10.1029/90GL02677 (1991).
[13]M. Berthomier, R. Pottelette, M. Malingre, and Y. Khotyaintsev, Phys. Plasmas **7**, 2987 (2000).
[14]R. E. Ergun, C. W. Carlson, J. P. McFadden, F. S. Mozer, L. Muschietti, I. Roth, and R. J. Strangeway, Phys. Rev. Lett. **81**, 826 (1998).
[15]J. R. Franz, P. M. Kintner, J. S. Pickett, and L.-J. Chen, J. Geophys. Res. **110**, 9212, DOI:10.1029/2005JA011095 (2005).
[16]M. Berthomier, R. Pottelette, L. Muschietti, I. Roth, and C. W. Carlson, Geophys. Res. Lett. **30**, 2148, DOI: 10.1029/2003GL018491 (2003).
[17]I. B. Bernstein, J. M. Greene, and M. D. Kruskal, Phys. Rev. **108**, 546 (1957).
[18]H. L. Berk, C. E. Nielsen, and K. V. Roberts, Phys. Fluids **13**, 980 (1970).
[19]K. Saeki, P. Michelsen, H. L. Pécseli, and J. J. Rasmussen, Phys. Rev. Lett. **42**, 501 (1979).
[20]V. L. Krasovsky, H. Matsumoto, and Y. Omura, J. Geophys. Res. **102**, 22131, DOI10.1029/97JA02033 (1997).
[21]L. Muschietti, R. E. Ergun, I. Roth, and C. W. Carlson, Geophys. Res. Lett. **26**, 1093, DOI:10.1029/1999GL900207 (1999).
[22]H. Schamel, Phys. Scr. **20**, 336 (1979).
[23]V. A. Turikov, Phys. Scr. **30**, 73 (1984).
[24]L.-J. Chen, J. Pickett, P. Kintner, J. Franz, and D. Gurnett, J. Geophys. Res. **110**, 9211, DOI:10.1029/2005JA011087 (2005).
[25]V. L. Krasovsky, H. Matsumoto, and Y. Omura, J. Geophys. Res. **108**, 1117, DOI:10.1029/2001JA000277 (2003).
[26]L. Muschietti, I. Roth, C. W. Carlson, and M. Berthomier, Nonlinear Processes Geophys. **9**, 101 (2002).
[27]M. V. Goldman, M. M. Oppenheim, and D. L. Newman, Geophys. Res. Lett. **26**, 1821, DOI:10.1029/1999GL900435 (1999).
[28]D. L. Newman, M. V. Goldman, M. Spector, and F. Perez, Phys. Rev. Lett. **86**, 1239 (2001).
[29]M. M. Oppenheim, D. L. Newman, and M. V. Goldman, Phys. Rev. Lett. **83**, 2344 (1999).
[30]N. Singh, Geophys. Res. Lett. **27**, 927, DOI:10.1029/1999GL003709 (2000).
[31]M. M. Oppenheim, G. Vetoulis, D. L. Newman, and M. V. Goldman, Geophys. Res. Lett. **28**, 1891, DOI:10.1029/2000GL012383 (2001).
[32]N. Singh, Nonlinear Processes Geophys. **10**, 53 (2003).
[33]N. Singh, S. M. Loo, and B. E. Wells, Geophys. Res. Lett. **28**, 1371, DOI:10.1029/2000GL012652 (2001).
[34]I. Roth, L. Muschietti, C. W. Carlson, F. S. Mozer, and R. E. Ergun, J. Geophys. Res. **107**, 1239, DOI:10.1029/2001JA900175 (2002).
[35]L. Muschietti, I. Roth, C. W. Carlson, and R. E. Ergun, Phys. Rev. Lett. **85**, 94 (2000).
[36]M. André, J. Atmos. Sol.-Terr. Phys. **59**, 1687 (1997).
[37]C. Beghin, J. L. Rauch, and J. M. Bosqued, J. Geophys. Res. **94**, 1359, DOI:10.1029/JA094iA02p01359 (1989).
[38]D. A. Gurnett, J. Geophys. Res. **71**, 5599 (1966).
[39]S. R. Mosier and D. A. Gurnett, J. Geophys. Res. **74**, 5675, DOI:10.1029/JA074i024p05675 (1969).
[40]H. G. James, J. Geophys. Res. **81**, 501, DOI:10.1029/JA081i004p00501 (1976).
[41]H. Lonnqvist, M. André, L. Matson, A. Bahnsen, L. G. Blomberg, and R. E. Erlandson, J. Geophys. Res. **98**, 13565, DOI:10.1029/93JA00639 (1993).
[42]R. E. Ergun, C. W. Carlson, J. P. McFadden, R. J. Strangeway, M. V. Goldman, and D. L. Newman, Phys. Plasmas **10**, 454 (2003).
[43]R. E. Ergun, M. V. Goldman, D. L. Newman, C. W. Carlson, J. P. McFadden, and R. J. Strangeway, Geophys. Res. Lett. **28**, 3805, DOI:10.1029/2001GL013024 (2001).
[44]N. Singh, Geophys. Res. Lett. **29**, 1833, DOI: 10.1029/2002GL015195 (2002).
[45]D. L. Newman, M. V. Goldman, and R. E. Ergun, Phys. Plasmas **9**, 2337 (2002).
[46]L.-J. Chen, D. J. Thouless, and J.-M. Tang, Phys. Rev. E **69**, 055401 (2004).
[47]M. Berthomier, L. Muschietti, J. W. Bonnell, I. Roth, and C. W. Carlson, J. Geophys. Res. **107**, 1463, DOI:10.1029/2002JA009303 (2002).
[48]L. D. Landau and E. M. Lifchitz, *Mechanics* (Mir, Moscow, 1964), p. 129.
[49]G. Vetoulis and M. Oppenheim, Phys. Rev. Lett. **86**, 1235 (2001).